Characterization of CuO:NiO/PS Hydrogen Gas Sensor

The 5th International scientific Conference on Nanotechnology& Advanced Materials Their Applications (ICNAMA 2015)3-4 Nov, 2015

Dr. Isam M. Ibrahim
College of Science, University of Baghdad/ Baghdad.
Email: yahya.rasheed1973@gmail.com
Yahya R. Hathal
College of Science, University of Baghdad/Baghdad.
Dr. Fuad T. Ibrahim
College of Science, University of Baghdad/Baghdad.
Dr. Mudhafar H. Ali
College of Science, University of Baghdad/Baghdad.

Abstract

Thin films of copper oxide nanoparticles mixed with 6% nickel oxide are deposited on glass and Si substrates with orientation (111) utilizing pulsed laser deposition technique for the manufacture of hydrogen gas sensor. The films are annealed in air at 400 °C for two hours, then the structural and morphological properties are characterized using x-ray diffraction and atomic force microscopy. The results of CuO:NiO/Si films are exhibited a polycrystalline monoclinic CuO and cubic NiO phases. In addition, the peak of Si located at 28.3º which refer to (111) direction. Furthermore, this peak becomes very broad with varying full width at half maximum for etching current density of 30 mA/cm^2 at time of 30 min which confirms the formation of pores on the crystalline silicon surface. On the other hand, the average diameter of 84.31 nm and 34.98 nm for CuO:NiO on a glass substrate and PS, respectively, were obtained. A sponge-like structure is produced for PS which reveal that a part of pores transform to a larger structure. The peak sensitivity of 204.8% was observed at optimum operating temperature of 350°C.

Keywords: Gas sensors, Pulsed Laser Deposition, Metal Oxides, Atomic Force Microscope

توصيف متحسس غاز الهيدروجين CuO:NiO/PS

الخلاصة

تم ترسيب جسيمات نانوية من أوكسيد النحاس مع 6% من أوكسيد النيكل على قواعد من الزجاج والسيليكون ذات اتجاهية (111) باستخدام تقنية الترسيب بالليزر النبضي لتصنيع متحسس لغاز الهيدروجين. تم تلدين الاغشية في الهواء عند درجة حرارة 400 درجة سيليزية، ثم دراسة الخواص التركيبية والسطحية باستخدام حيود الاشعة السينية ومجهر القوى الذرية. أظهرت نتائج الاغشية لأوكسيد النحاس مع أوكسيد النيكل على السيليكون بأن الغشاء يمتلك طور متعدد التبلور احادي الميل لأوكسيد النحاس وطور مكعب لأوكسيد النيكل. بالإضافة الى قمة السيليكون عند الزاوية 28.3 درجة والذي يشير الى الاتجاه (111). علاوة على ذلك، هذه القمة تصبح عريضة جدا مع تغير عرض المنحني عند منتصف القمة لكثافة تيار 30 ملي امبير/سنتيمتر مربع وخلال زمن 30 دقيقة والذي يؤكد تشكل المسامات على سطح السيليكون المسامي. من ناحية اخرى، تم الحصول على معدل القطر 84.31 نانومتر و34.98 نانومتر لأوكسيد النحاس مع اوكسيد النيكل على قواعد من الزجاج والسيليكون المسامي على الترتيب. الشكل الاسفنجي الناتج للسيليكون المسامي يشير الى أن جزء من المسامات

تحولت الى بنية اكبر. أعلى تحسسية 204.8% تم الحصول عليها عند درجة الحرارة المثالية والتي تساوي 350°C.

الكلمات المفتاحية : متحسسات الغاز- الترسيب بالليزر النبضي - أكاسيد المعادن- مجهر القوى الذرية.

INTRODUCTION

Oxide semiconductors have been used to detect oxidizing and reducing gases in simple and cost-effective have manner [1]. Their chemiresistive variation emanates from the oxidative or reductive interaction of the analytic gas with the oxide semiconductor surface and the consequent change in the charge carrier concentration. In p-type oxide semiconductor gas sensors such as those comprising CuO, NiO, Co_3O_4 and Cr_2O_3, the adsorption of negatively charged oxygen forms a hole accumulation layer near the surface. Thus, conduction occurs along the conductive hole accumulation layer [2].

Sensors are devices that produce a measurable change in output in response to a specified input stimulus [3]. This stimulus can be a physical stimulus like temperature and pressure or a concentration of a specific chemical or biochemical material. The output signal is typically an electrical signal proportional to the input variable. Sensors can be used in all three phases of matter although gas and liquid sensors are the most common [4]. Transparent conducting thin films are a class of material which achieve large values of electrical conductivity, whilst maintaining a high transmission in the visible range of the electromagnetic spectrum [5].

Hydrogen gas is tasteless, colorless and odorless so it cannot be detected by human beings. The low ignition energy and wide flammable range make it easy inflammable and explosive. Therefore, rapid and accurate hydrogen detection is necessary during the production, storage and use of hydrogen and it is also essential for monitoring/controlling the hydrogen concentration of nuclear reactors, coal mines and semiconductor manufacturing [6].

Studies on copper oxide nanomaterial have grown substantially in recent years due to its direct band gap and intrinsic p-type behavior together with low cost fabrication and good electrochemical properties. Copper oxide shows two types of polymorphism, namely, cuprous oxide Cu_2O and cupric oxide CuO which can be considered as the most important stoichiometric compounds in the CuO system. Pure cupric oxide is a black solid with a density of 6.4 g/cm^3. It also has a high melting point of 1330 ºC and is insoluble in water. CuO is intrinsic p-type semiconductors with relatively small band gap of 1.2-1.85 eV and show many attractive properties that can be utilized in a diversity of applications. Copper oxides are used for gas sensors for hydrogen and volatile organic compounds [7]. catalysis and specially, cuprous oxide films were intensively researched in device applications such as photovoltaic solar cell [8] photo electrochemical cell and electro-chromic coatings. Based on its application and interesting physical properties its synthesis has become important. Therefore, a wide range of deposition techniques such as chemical vapor deposition, electro deposition, thermal evaporation, sol-gel techniques, spray pyrolysis and pulsed laser deposition have been demonstrated [9].

Nickel oxide NiO is p-type semiconductor material and is widely used in different applications such as transparent conductive films, electro-chromic devices , as a potential candidate in the chemical sensors. NiO exhibits a wide band gap of 3.6–4.0 eV at room temperature; thus, NiO is considered transparent in the visible light region. Moreover, NiO is largely used as a catalyst with different n-type semiconductors due its high p-type concentration, high hole mobility and low cost.

The existence of NiO enhances the separation of electron and hole pairs via electric junction field and also promotes the interfacial charge transfer [10].

Experimental

Copper oxide nanoparticles with 6% of nickel oxide was prepared utilizing pressure of 5 ton to form a target with a diameter of 1.5 cm and thickness of 0.2 cm. It should be dense as well as homogeneous to obtain the best quality of the deposit. The experiment is achieved under vacuum chamber conditions of 10^{-3} Torr. The laser beam is incident through a window and focused on the target surface to make an angle of 45° with the sample. The substrate is put in parallel versus the target in which a suitable gap is saved. Furthermore the holder of substrate the substrate did not block the incident laser beam. This deposition technique has been modified in order to obtain films with better quality which comprise rotation of the target according to the position of substrate as shown in Figure (1).

.

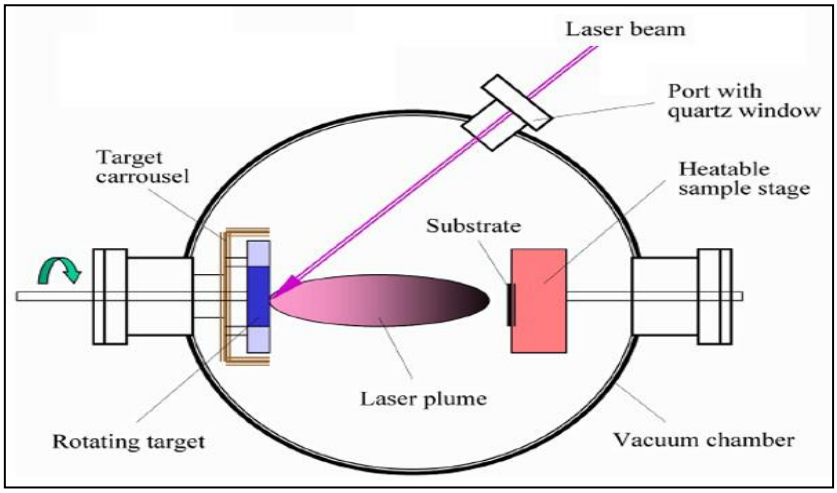

Figure (1) Schematic of a PLD chamber

Porous silicon prepared by electrochemical etching were the silicon wafer serves as the anode. The cathode is made of platinum or any HF-resistant and conducting material. The cell body itself is, in general, made of highly acid-resistant polymer such as Teflon. Si wafer p-type (111) was used as a starting substrate in the electrochemical etching. The samples were cut from the wafer and rinsed with acetone and methanol to remove dirt. In order to remove the native oxide layer on the samples, they were etched in diluted HF acid (1:1) with etching current 30 mA and time 30 min as shown in Figure (2).

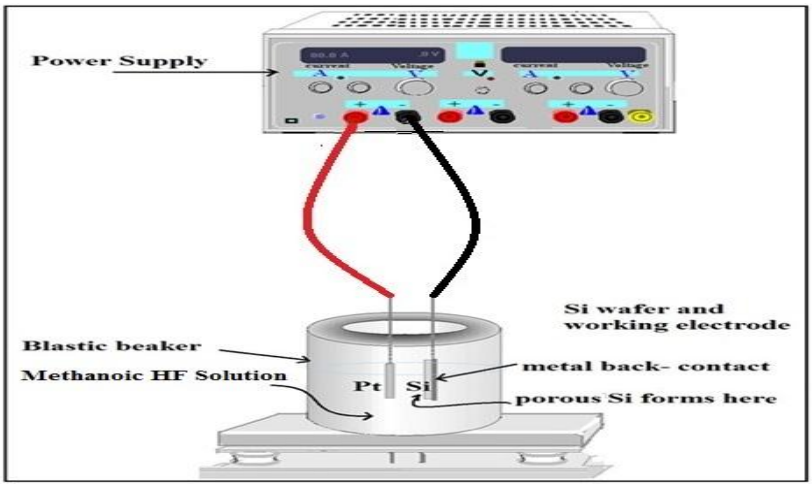

Figure (2) A photo of the porous silicon testing system

Result and discussion:

Results and discussion include structural and morphological analysis

Structural analysis:

The XRD analyses have been done by using "SHIMADZU" XRD-6000 X-ray diffract meter (CuKα radiation λ=0.154nm) in 2θ range from 20° to 60°. Figure (3) shows the x-ray diffraction patterns of deposited CuO thin films prepared by pulse laser deposition (PLD) technique with 6% NiO on a Si (111) wafer. We can observe the peak of Si located at about 28.3º which related (111) direction. At 6 % NiO content there are four peaks located at (2θ = 35.55º and 38.85º) referred to {(11$\bar{1}$) and (111)} direction for CuO crystals, while at (2θ =36.50º and 42.86º) referred to {(111) and (200)} direction respectively for NiO crystals. The x-ray diffraction data of thin films identical with that of known CuO monoclinic structure and NiO cubic structure according to the International center for diffraction card No. (96-410-5686) and (96-432-0506). The preferred peak for films appear at (11$\bar{1}$) plane for CuO.

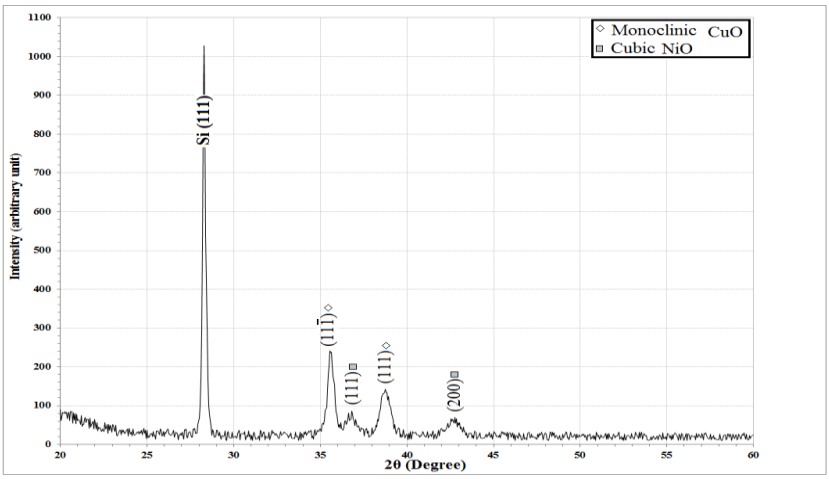

Figure (3) x-ray diffraction patterns for CuO films with 6% NiO content.

Table (1) shows a comparison between experimental and standard peaks from International Centre for Diffraction.

Table (1) comparison between experimental and standard values of x-ray diffraction peaks for CuO films with 6% NiO content.

NiO%	2θ (Deg.)	FWHM (Deg.)	d_{hkl} Exp.(Å)	G.S (nm)	d_{hkl} Std.(Å)	Phase	hkl	Card No.
6	35.6012	0.4111	2.5197	20.3	2.5216	CuO	$(11\bar{1})$	96-410-5686
	36.7756	0.7215	2.4419	11.6	2.4254	NiO	(111)	96-432-0506
	38.7599	0.6313	2.3214	13.3	2.3158	CuO	(111)	96-410-5686
	42.7283	0.8568	2.1145	10.0	2.1005	NiO	(200)	96-432-0506

XRD studies for PS showed distinct variations between the wafer silicon surface and the porous silicon surface formed at etching current 30 mA with etching time 30 min. When crystal size is reduced toward nanometric scale, then a broadening of diffraction peak is observed and the width of the peak is directly correlated to the size of the nano crystalline domains[11,12]. XRD spectra of wafer silicon showed a very sharp peak at 2θ = 28.391° showing the single crystalline nature of the wafer. This peak becomes very broad with varying full width at half maximum (FWHM) which confirms the formation of pores on the crystalline silicon surface as shown in Figure (4).

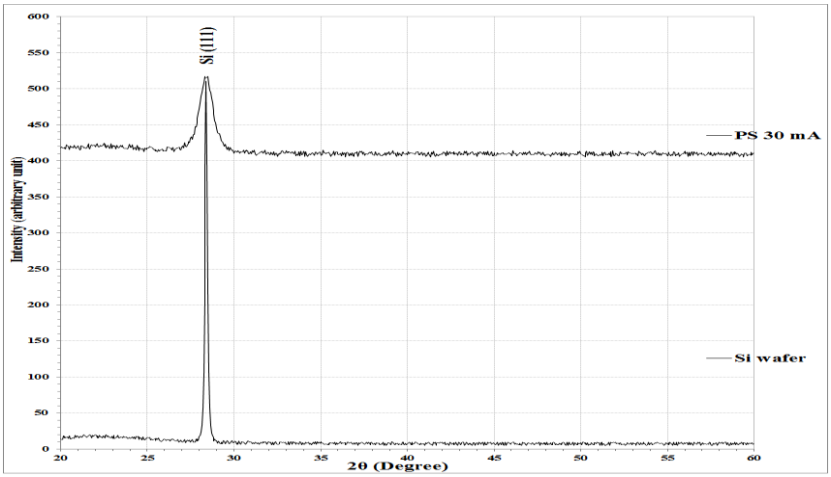

Figure (4) X-ray diffraction patterns for Si wafer and PS.

Table (2) shows the effect of etching current on Si wafer, this peak becomes very broad were the full-width at half maximum increases, i.e. decrease the grain size, as a result of porosity.

Table (2) comparison between experimental and standard values of x-ray diffraction peaks for Si wafer and Porous Si with etching current 30 mA and time 30 min.

Sample	2θ (Deg.)	FWHM (Deg.)	d_{hkl} Exp.(Å)	G.S (nm)	d_{hkl} Std.(Å)	hkl
Si wafer	28.3914	0.1820	3.1411	45.0	3.1474	(111)
30 mA	28.3765	0.9050	3.1427	10.1	3.1474	(111)

Morphological analysis:

The atomic force microscopy (AFM) were taken for CuO:NiO on glass substrates and PS by AA3000 Scanning Probe Microscope Angstrom Advanced Inc. Figure (5) shows the atomic force microscopy (AFM) image for CuO with 6 % now content deposited on a glass substrate. AFM parameters (average diameter, average roughness and peak –peak) for the sample have been shown in Table (3).

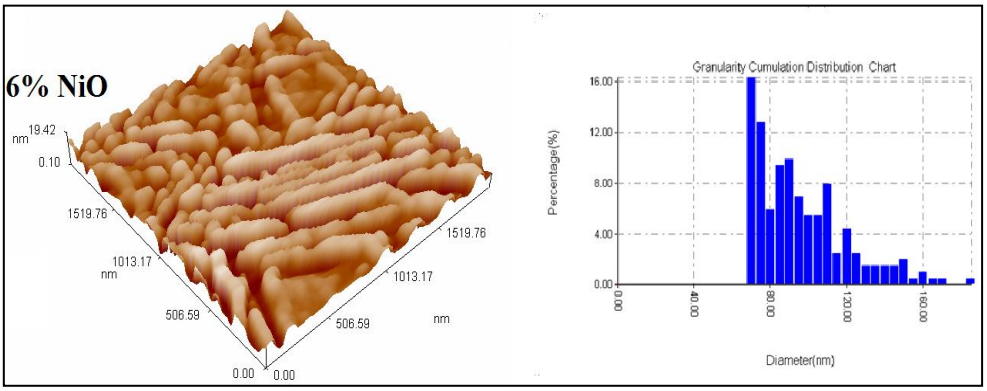

Figure (5) Atomic force microscopy for CuO with 6%NiO content deposited on glass.

Table (3) AFM parameters for CuO film with 6%NiO content deposited on a glass substrate.

NiO%	Avg. Diameter(nm)	Avg.Roughness(nm)	Peak-peak(nm)
6	84.31	1.3	8.45

Figure (6) shows AFM image of porous silicon at time of 30 min and etching current of 30 mA. When current flows in the electrochemical cell, the dissociation reaction localizes on a particular side of a silicon surface, thus initiating the etching of an array of pores in the silicon wafer. The pore morphology was analyzed under conditions of varying current densities. At low current density, a highly branched, randomly directed and highly interconnected meshwork of pores was obtained. However, increasing in current density orders the small pores to exhibit cylindrical shapes giving rise to larger pore diameter [12]. AFM parameters average diameter, average roughness and (peak –peak) for the sample has been shown in table (4).

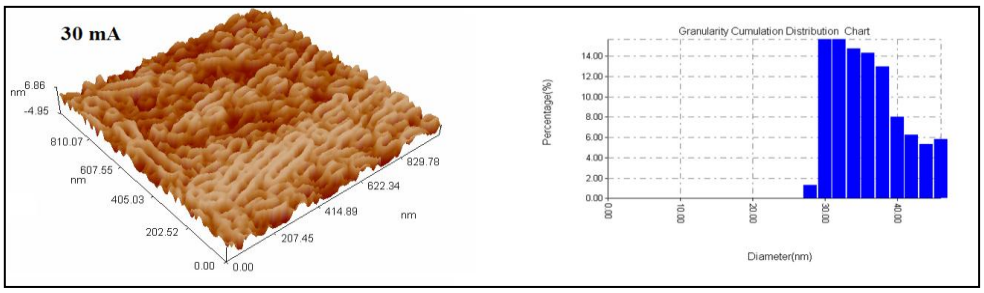

Figure (6) Atomic force microscopy for porous silicon with time 30 min and etching current of 30 mA.

Table (4) AFM parameters for PS with etching current of 30 mA and time of 30 min.

Current (mA)	Avg. Diameter(nm)	Avg. Roughness(nm)	Peak-peak(nm)
30 mA	34.98	1.49	5.98

Gas Sensing Measurement:

Figure (7) exhibits the sensitivity versus the operating temperature from RT to 350 °C for, at etching current of 30 mA and deposited on porous Si wafer (111). During the experiment the hydrogen gas concentration was kept constant of 5 % in atmospheric air. The results show an increment in sensitivity with the increasing of operating temperature wherein the maximum value of 204.8% was observed at 350°C. In other words, the highest sensitivity was obtained at the optimum operating temperature 350°C for this sensor.

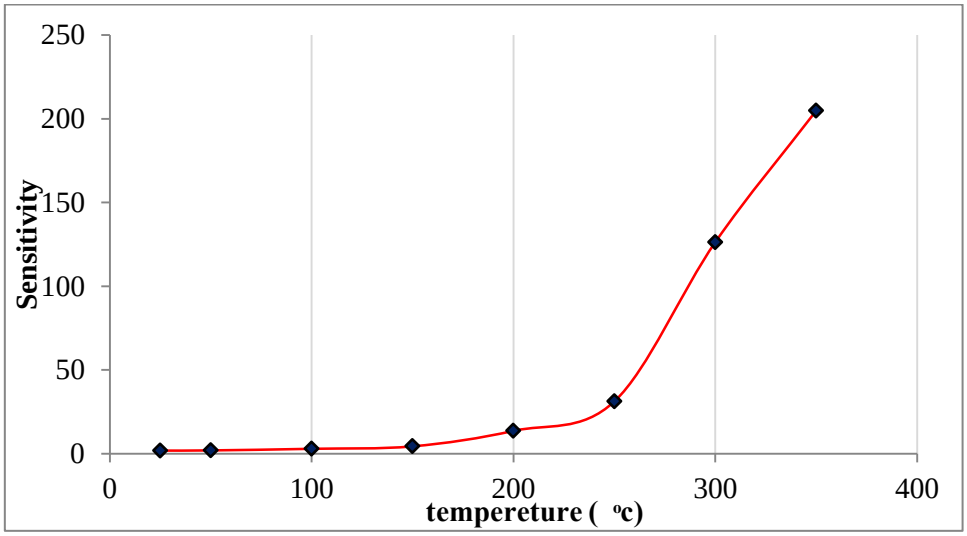

Figure (7) The sensitivity as a function of operating temperature at etching current of 30 mA for CuO with 6% NiO content on PS.

Figure (8) Illustrates the sensitivity as a function of time at optimum operating temperature of 350°C. Four hydrogen / air mixing ratios are used in this part 5%, 10%, 15% and 20%. The results show an increment in sensitivity of the gas sensor with the increasing of hydrogen air mixing ratio. The peak sensitivity of 318% was obtained at the ratio of 20% . The sensitivity tends to saturate in the high gas concentration . It can be concluded that the sensitivity is directly proportional to the hydrogen / air mixing ratio [13].

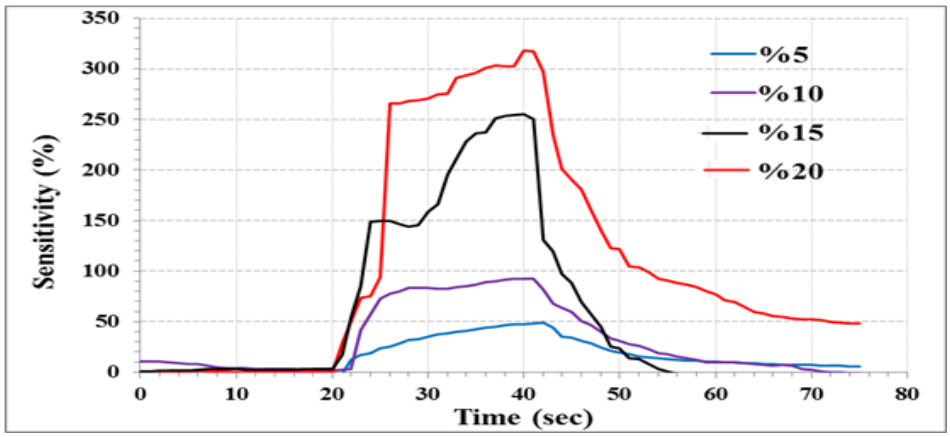

Figure (8) The sensitivity as a function of time for different hydrogen / air mixing ratio.

Figure (9) exhibits the response time and recovery time as a function of operating temperature for CuO:6%NiO nano film. The best response speed of 6.3 sec and recovery time of 12.6 sec were obtained at operating temperature of 150 and 200 °C.

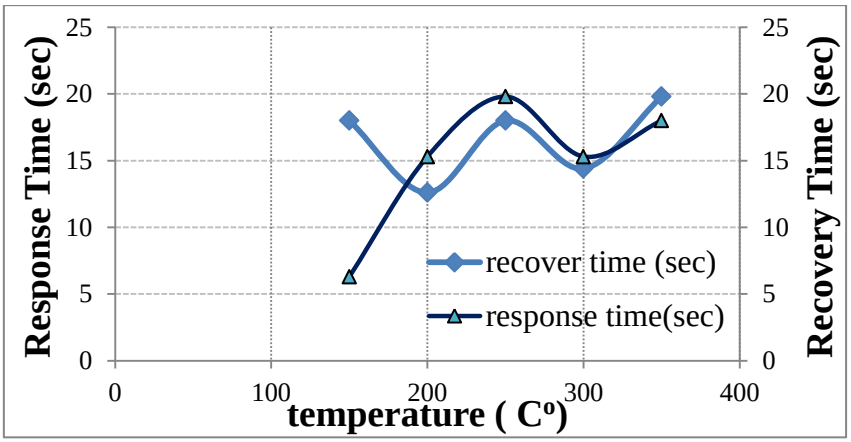

Figure (9) The variation of response time and Sensitivity with the operating temperature for CuO:6%NiO/PS at etching current 30 mA.

Conclusions:

1. The CuO:6%NiO polycrystalline thin films based pulsed laser deposition technique were successfully prepared.
2. The XRD properties showed the porous structure and the decrease of the Si nano-sized because a broadening of the Si peak.
3. The atomic force microscopy images show the increment in the roughness of silicon surface with increasing of etching current.
4. The porous Si gas sensor works at higher temperature up to 350 °C.
5. Increasing in concentration hydrogen testing gas lead to increasing in sensitivity at optimal operating temperature.

References:

[1] N. Yamazoe, "Toward innovations of gas sensor technology," in Sensors and Actuators, B: Chemical, 2005, vol. 108, pp. 2–14.
[2] S. Pokhrel, C. E. Simion, V. Quemener, N. Bârsan, and U. Weimar, "Investigations of conduction mechanism in Cr2O3 gas sensing thick films by ac impedance spectroscopy and work function changes measurements," Sensors Actuators, B Chem., vol. 133, pp. 78–83, 2008.
[3] J. R. Stetter and W. R. Penrose, "Understanding Chemical Sensors and Chemical Sensor Arrays (Electronic Noses): Past, Present, and Future," Sensors Updat., vol. 10, pp. 189–229, 2002.
[4] C. Wagner, "The mechanism of the decomposition of nitrous oxide on zinc oxide as catalyst," J. Chem. Phys, vol. Vol. 18, no. No.1, pp. pp. 69 – 71, 1950.
[5] P. P. Edwards, A. Porch, M. O. Jones, D. V Morgan, and R. M. Perks, "Basic materials physics of transparent conducting oxides.," Dalton Trans., pp. 2995–3002, 2004.
[6] H. Gu, Z. Wang, and Y. Hu, Hydrogen Gas Sensors Based on Semiconductor Oxide Nanostructures, vol. 12. 2012, pp. 5517–5550.
[7] D. Barreca, E. Comini, A. Gasparotto, C. Maccato, C. Sada, G. Sberveglieri, and E. Tondello, "Chemical vapor deposition of copper oxide films and entangled quasi-1D nanoarchitectures as innovative gas sensors," Sensors Actuators, B Chem., vol. 141, pp. 270–275, 2009.
[8] L. M. Wong, S. Y. Chiam, J. Q. Huang, S. J. Wang, J. S. Pan, and W. K. Chim, "Growth of Cu[sub 2]O on Ga-doped ZnO and their interface energy alignment for thin film solar cells," J. Appl. Phys., vol. 108, p. 033702, 2010.
[9] "Synthesis and Characterization of CuO / graphene oxide composite National Institute of Technology , Rourkela," no. 411, pp. 2012–2013, 2013.
[10] Z. H. Ibupoto, M. A. Abbasi, X. Liu, M. S. Alsalhi, and M. Willander, "The synthesis of NiO/TiO_2 heterostructures and their valence band offset determination," J. Nanomater., vol. 2014, 2014.
[11] A. Lorusso, V. Nassisi, G. Congedo, N. Lovergine, L. Velardi, and P. Prete, "Pulsed plasma ion source to create Si nanocrystals in SiO2 substrates," Appl. Surf. Sci., vol. 255, pp. 5401–5404, 2009.
[12] L. Russo, F. Colangelo, R. Cioffi, I. Rea, and L. De Stefano, "A mechanochemical approach to porous silicon nanoparticles fabrication," Materials (Basel)., vol. 4, pp. 1023–1033, 2011.
[13] S. N. Das, J. P. Kar, J.-H. Choi, T. Il Lee, K.-J. Moon, and J.-M. Myoung, "Fabrication and Characterization of ZnO Single Nanowire-Based Hydrogen Sensor," J. Phys. Chem. C, vol. 114, pp. 1689–1693, 2010.